Insights into the Mechanism of Cumene Peroxidation Using Supported Gold and Silver Nanoparticles

Charles-Oneil L. Crites,[†] Geniece L. Hallett-Tapley,[†] Mathieu Frenette,[†] María González-Béjar,[†,‡] J. C. Netto-Ferreira,*[,†,§] and J. C. Scaiano*[,†]

[†]Department of Chemistry and Centre for Catalysis Research and Innovation, University of Ottawa, 10 Marie Curie, Ottawa K1N 6N5, Canada

[‡]Instituto de Ciencia Molecular, Departamento de Química Orgánica, Universidad de Valencia, C/Catedrático José Beltrán, 2, 46980, Paterna, Valencia, Spain

[§]Departamento de Química, Universidade Federal Rural do Rio de Janeiro, Seropédica, 23851-970, Rio de Janeiro, Brazil

Ⓢ *Supporting Information*

ABSTRACT: Due to the considerable industrial implications, an in-depth study of cumene peroxidation using supported gold and silver nanoparticles was carried out to gain more insight into the mechanism of this reaction. Supported gold nanoparticles were found to efficiently catalyze the decomposition of cumene hydroperoxide with a selectivity of 25% at 80 °C when using gold supported on hydrotalcite (AuNP@HT), and 2-phenyl-2-propanol (i.e., cumyl alcohol) was the main product. Further, silver nanoparticles supported on hydrotalcite (AgNP@HT) converted cumene to cumene hydroperoxide at 80 °C with 80% selectivity. Both benchtop and oxygen-uptake experiments were used to probe the reaction mechanism and suggest that formation of a peroxyl radical-nanoparticle adduct is an important step in the peroxidation pathway and may be directly involved in the formation of the major cumyl alcohol product.

KEYWORDS: *oxidation, free radicals, heterogeneous catalysis, hydrotalcite, nanotechnology, Hock rearrangement*
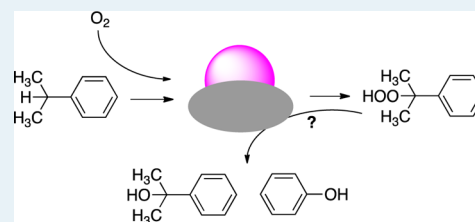
INTRODUCTION

Oxidation reactions are one of the most fundamental reactions on the industrial level. Notably, free-radical reactions are used to synthesize several chemicals, including cyclohexane hydroperoxide, ethylbenzene hydroperoxide, and cumene hydroperoxide. These hydroperoxides are important intermediates in several industrial processes.[1] In particular, cumene hydroperoxide accounts for the vast majority of the world production of acetone and phenol. Considerable efforts have focused on the catalytic formation of hydroperoxides. Ethylbenzene hydroperoxide is a key intermediate in the Halcon process, commonly formed by the metal salt catalyzed free-radical oxidation of tetraline in the 1950s and 1960s.[2,3] Later, heterogeneous materials, notably MnO_2 and Cu_2O,[4] were used in the free-radical oxidation of cumene. More recently, nanostructures have been investigated as potential alternative catalysts in hydroperoxidations. One of the more recent examples involves ethylbenzene oxidation using NiAl hydrotalcite catalysts, also thought to proceed *via* a free-radical mechanism.[5] In many cases, the catalytic process can be viewed as a desirable perturbation of the well-established autoxidation of reactions 1–4.
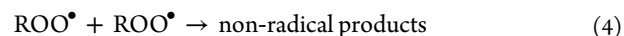
Initiation:

$$\text{production of } R^\bullet, ROO^\bullet, \text{ or } RO^\bullet \tag{1}$$

Propagation:

$$R^\bullet + O_2 \rightarrow ROO^\bullet \tag{2}$$

$$ROO^\bullet + HR \rightarrow ROOH + R^\bullet \tag{3}$$

Termination:

$$ROO^\bullet + ROO^\bullet \rightarrow \text{non-radical products} \tag{4}$$

The initiation (eq 1), the propagation (eqs 2 and 3), and the termination (eq 4) are steps that occur in a typical free radical chain reaction.

Although formation of hydroperoxides through the use of a variety of catalysts has been demonstrated,[6] a major disadvantage that still remains relates to the instability of hydroperoxides in the presence of the catalyst.[7] Typically, the hydroperoxide will decompose into the corresponding alcohol. This pathway can sometimes be useful, as in the case of cyclohexane oxidation to cyclohexanol,[8–11] an important step in the formation of caprolactam, the major precursor for the synthesis of Nylon-6.

Also of considerable importance is the Hock rearrangement from cumene hydroperoxide to phenol and acetone, highly sought-after in the chemical industry.[12] However, several

studies examining the formation of cumene hydroperoxide using silver nanoparticles on Al_2O_3,[13] as well as copper and copper oxide nanoparticles[14] on MgO,[15] have shown that the undesired cumyl alcohol was obtained in significant yields. Further studies by Lloyd et al.[16] using supported gold nanoparticles have demonstrated the importance of the support toward hydroperoxide stability. Silver nanoparticles (AgNP) have been shown to catalyze the peroxidation of cumene, even though the influence of the support in these reactions was not conclusive.[6] More so, the work of Van Ham et al.[13] demonstrates that AgNP, under oxygen, does not degrade cumene hydroperoxide but still catalyzes cumene peroxidation.

From the literature, it is evident that some supported nanoparticle catalysts strongly influence the stability of hydroperoxides, as well as that of common radical initiators.[17,18] Due to the sheer importance of cumene hydroperoxide, this contribution will focus mainly on this intermediate and is aimed at examining the use of potential heterogeneous nanoparticle catalysts, specifically supported AuNP and AgNP, not only to maximize cumene hydroperoxide production but also to reduce the yield of the cumyl alcohol byproduct, formed *via* hydroperoxide degradation.

Clearly, some catalysts and their supports can influence the stability of the hydroperoxide, a product of the reaction, but also play an important role as a radical initiator. This work was undertaken with two questions in mind:

Do typical oxidation catalysts induce the decomposition of typical oxidation initiators, in particular hydroperoxides?

Do oxidation catalysts influence, in any way (catalysis or inhibition), the free-radical chain reaction that mediates oxidation?

To the best of our knowledge, these questions have not been addressed in any detail in earlier work, especially when considering supported AuNP; yet, we believe that understanding these issues is key to mechanistic proposals dealing with the catalytic oxidation of alkenes (leading to epoxides), as catalyst-induced initiator decomposition will have significant effects on both the kinetics and efficiency of such reactions. Most work was carried out at low conversions to reveal the early stages of the oxidation process. Clearly, it would be impossible to address questions *i* and *ii* for all combinations examined in the literature. We simply aim at addressing these issues for some key systems, notably some widely employed supported gold nanoparticles, such as commercially available AuNP@TiO₂. This work also allows the opportunity to study the formation of cumene hydroperoxide, which is made *via* the autoxidation of cumene in a process that is not catalyzed in industry.[19]

■ EXPERIMENTAL SECTION

Reagents. Cumene, cumene hydroperoxide (CHP; technical grade 80%, largely cumene impurity), cumyl alcohol (98%; 2-phenyl-2-propanol), acetophenone (98%), dicumyl peroxide (DCP; 97%), 2,6-di-*tert*-butyl-4-methoxyphenol (95%, DBHA), *tert*-butyl hydroperoxide solution in H_2O (80%), and dodecane (99%), chlorobenzene (99.5%), hydrotalcite (HT), sodium borohydride ($NaBH_4$), tetrachloroauric acid ($HAuCl_4·H_2O$), silver nitrate, phenol, lipoic acid (99%), and optima grade acetonitrile were purchased from Sigma-Aldrich and used as received. TiO_2 P25 was a gift from Evonik Degussa. AUROlite 1% AuNP@TiO₂ was purchased from Strem Chemicals and was ground using a mortar and pestle prior to use. The average size of the AuNP was determined to be 2.3 nm by TEM (Figure S1, Supporting Information). Optima grade heptane, 2-

propanol, and ammonia (28% in H_2O) were purchased from Fisher Chemicals and used as received. Millipore H_2O was deionized in house (18.2Ω at 25 °C) and used in the synthesis of supported metal nanoparticles.

Instruments. The size of the metallic nanoparticles was determined using a JEM-2100F FETEM transmission electron microscope (TEM) from Jeol Ltd. Analysis of the reaction mixture (cumyl alcohol, acetophenone, and cumene hydroperoxide) was carried out using a normal phase Agilent 1100 HPLC (eluent 99:1 heptane/2-propanol). The amount of dicumyl peroxide was determined using a Waters HPLC fitted with a reverse phase C-18 silica column and employing an eluent mixture of 60:40 acetonitrile/water. Representative reverse and normal phase HPLC spectra are shown in Figures S4–S6, Supporting Information. Experiments requiring controlled gas flow used a Matheson flow meter.

Synthesis of Supported Gold Nanoparticles on Hydrotalcite (AuNP@HT). The procedure was adapted from previous work by Mitsudome et al.[20] A total of 2 g of hydrotalcite was added to 60 mL of an aqueous solution of 1.8 mM $HAuCl_4·H_2O$. A total of 0.09 mL of a 10% solution of NH_4OH was added after several minutes, and the mixture was allowed to stir overnight. The supported Au^{3+} composite was filtered, washed with water, and resuspended in water, and 10 mL of a 200 mM solution of sodium borohydride was added and allowed to react for 2 h. Finally, the purple solid was filtered, washed with water, and dried under ambient conditions. The theoretical loading was 1%, and the average nanoparticle size was determined to be 5.8 nm by TEM (see Figure 1 and S2, Supporting Information).
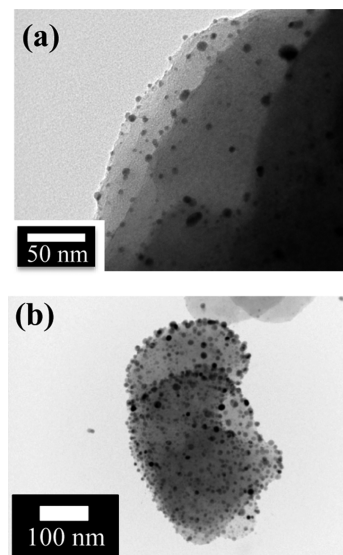

Figure 1. Representative TEM images of (a) AuNP@HT and (b) AgNP@HT.

Synthesis of Supported Silver Nanoparticles on Hydrotalcite (AgNP@HT). The procedure was adapted from previous work from Mitsudome and co-workers.[21] A total of 2 g of hydrotalcite was added to 60 mL of an aqueous solution of 2.9 mM silver nitrate. The solution was cooled using an ice bath and purged with nitrogen. After stirring for 4 h, the Ag^+/hydrotalcite composite was filtered, washed, and resuspended in water. Under a nitrogen atmosphere, 10 mL of a 200 mM solution of sodium borohydride was added to the slurry.

The yellow solid was then filtered and washed with water and dried at ambient temperature. The theoretical loading was calculated to be 1%, and the average nanoparticle size was determined to be 10 nm by TEM (see Figures 1 and S3, Supporting Information).

Peroxidation of Cumene under Atmospheric Conditions. In a 50 mL, two-neck round-bottom flask, 200 mg of catalyst and 12 μL (0.05 mmol) of an aqueous solution of *tert*-butyl hydroperoxide were added to 20 mL of cumene and the reaction heated to 80 °C. This corresponds to 0.035% equivalents of initiator; note that conversions are low and that the reaction generates hydroperoxides that also act as initiators. An aliquot was taken from the reaction mixture every hour, centrifuged, and subsequently analyzed *via* HPLC. Control reactions were carried out using the support itself and in the absence of heterogeneous materials (*tert*-butyl hydroperoxide initiator only).

Peroxidation of Cumene under Oxygen Saturated Conditions. The experimental protocol is the same as that used for the reactions under atmospheric conditions. However, oxygen was continuously bubbled into the solution using a Teflon needle in order to prevent contamination by iron. The oxygen flow was controlled using a flow regulator.

Decomposition of Cumene Hydroperoxide (CHP) in Dodecane. In a 50 mL, two-neck flask, 200 mg of catalyst and 500 μL of an 80% solution of cumene hydroperoxide were added to 20 mL of dodecane, and the reaction was heated to 80 °C. An aliquot was taken from the reaction mixture every hour, centrifuged, and then analyzed *via* HPLC. Control reactions were also carried out as indicated in the procedure for the peroxidation of cumene under O_2.

Oxygen Uptake Experiments. The oxygen uptake apparatus was a gift from Prof. Ross Barclay of Mount Allison University (Sackville, NB). This system, built in-house, monitors small pressure differences between two samples (sensitivity <100 nmol O_2). Technical details of the design are presented elsewhere.[22,23] The amount of oxygen consumed was determined by measuring the change in the pressure difference between the reference and the reaction cell. Oxygen uptake experiments were carried out at 30 °C due to technical limitations of the instrument.

The experiments were conducted as follows: 5 mL of cumene was added to the reference and reaction cells, and then 12.6 mg of the catalyst of interest was added to the reaction cell. To initiate the reaction, 100 μL of a 176 mmol aqueous solution of *tert*-butyl hydroperoxide was added to the reaction cell. The rate of propagation is determined by graphical measurements and corresponds to the first derivative of the amount of oxygen produced with time.

Oxygen Uptake Experiments: Determining the Rate of Initiation (R_i). The same general procedure described in the preceding section was used; however after measuring the rate of propagation, 100 μL of an 8.0 mmol solution of 2,6-di-*tert*-butyl-4-methoxyphenol antioxidant was added in order to determine the inhibition period due to trapping of radical species. This inhibition period provides information about the rate of initiation, which corresponds to the rate at which free radicals are formed from nonradical precursors.[24]

Recyclability Experiments. In a 50 mL, two-neck round-bottom flask, 200 mg of catalyst and 12 μL (0.05 mmol) of an aqueous solution of *tert*-butyl hydroperoxide were added to 20 mL of cumene and the reaction heated to 80 °C for a period of 8 h. After reaction, the slurry was transferred to glass centrifuge

tubes and centrifuged at 3000 rpm for 15 min. The catalyst was separated from the reaction mixture and washed three times using CH_3CN to remove any adsorbed organics from the composite surface.

Peroxidation Inhibition Using 2,6-di-*tert*-butyl-4-methoxyphenol (DBHA) and AuNP Surface Functionalization Using Lipoic Acid. In a 50 mL, two-neck round-bottom flask, 100 mg of catalyst and 7 μL (0.025 mmol) of an aqueous solution of *tert*-butyl hydroperoxide were added to 10 mL of cumene and the reaction heated to 80 °C for a period of 3 h. An aliquot was taken every 30 min, centrifuged, and subsequently analyzed *via* HPLC. Either 100 mg of 2,6-di-*tert*-butyl-4-methoxyphenol or 5 mg of lipoic acid was added after 1 h to observe the effects on the overall product yields.

■ RESULTS

The TEM image of AuNP@HT, shown in Figure 1a, illustrates an average NP size of 5.8 ± 2.7 nm. Likewise, Figure 1b presents a representative TEM image for AgNP@HT and average particle sizes of 10.0 ± 3.2 nm. The corresponding size distribution histograms are presented in Figures S2 and S3. Additionally, the TEM of the commercial AuNP@TiO$_2$ can be seen in Figure S1.

Commercial AuNP@TiO$_2$ as a Catalyst for Cumene Peroxidation. Our initial goal was to study cumene peroxidation using commercially available AuNP supported on TiO$_2$ in the presence of a *tert*-butyl hydroperoxide initiator. As illustrated in Figure 2, when the reaction is performed in the
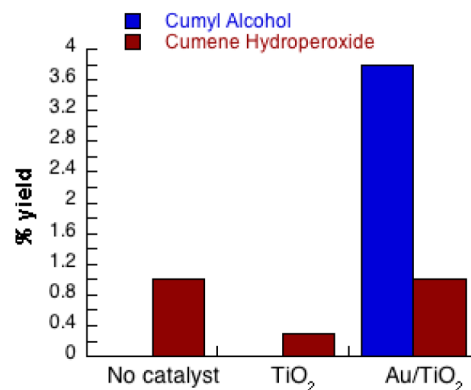

Figure 2. Bar graph illustrating the yield of cumyl alcohol and cumene hydroperoxide after 24 h when using no catalyst, TiO$_2$, and commerical AuNP@TiO$_2$ at 80 °C and *tert*-butyl hydroperoxide as an initiatior.

absence of a nanoparticle catalyst, a 1.0% yield of cumene hydroperoxide (CHP) was obtained after 24 h of reaction. When the support alone (TiO$_2$) was used, minimal yields of cumene hydroperoxide were observed. On the other hand, using commercial AuNP@TiO$_2$ as the catalyst, yields of 3.8% for cumyl alcohol and 1.0% for cumene hydroperoxide were obtained. The different product distributions obtained when using the support alone and the nanomaterial indicate that TiO$_2$ alone is not capable of cumene hydroperoxide decomposition into cumyl alcohol via a free-radical pathway.[25]

The reaction kinetics using commercial AuNP@TiO$_2$ (Figure 3) monitored over 8 h clearly show that cumene hydroperoxide is not detected before 3 h of reaction and that cumyl alcohol is the major product obtained.
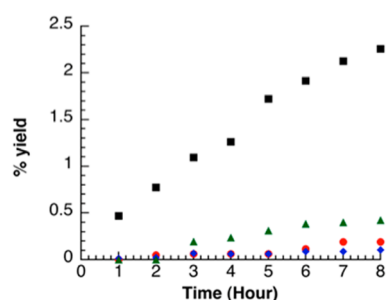
Figure 3. Percent yield of cumyl alcohol (■), CHP (●), acetophenone (♦), and DCP (▲) obtained for the peroxidation of cumene using commerical AuNP@TiO$_2$ at 80 °C over 8 h.

Other secondary products were obtained in small quantities when commercial AuNP@TiO$_2$ was used as a peroxidation catalyst (Figure 3). Acetophenone was formed from a secondary radical pathway involving β-scission of the cumyloxyl radical, while dicumyl peroxide (DCP) resulted from the recombination of two cumyl peroxyl radicals or two cumyloxyl radicals (Scheme 1). Notably, cumene peroxidation control

Scheme 1. Formation of Secondary Products for Cumene Peroxidation Using Commercial AuNP@TiO$_2$: (a) Formation of Acetophenone via β-Scission, (b) Formation of DCP via Radical Recombination of Two Cumyloxyl Radicals, and (c) Formation of DCP via Recombination of Two Cumyl Peroxyl Radicals
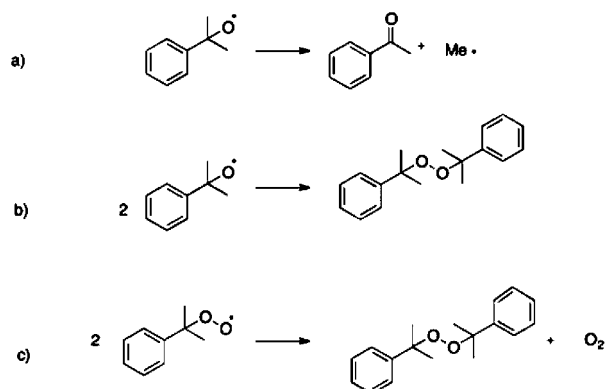
experiments run in the absence of catalyst or using TiO$_2$ alone yielded only trace amounts of product (Figures S7 and S8, Supporting Information).

Figure 4 illustrates the decomposition of CHP as a function of % CHP remaining. The objective of this experiment is to determine the stability of cumene hydroperoxide under different reaction conditions. In each case, CHP and the catalyst were added to dodecane, a solvent relatively inert toward radical processes.[26] As can be seen, in the absence of a catalyst, the percentage of CHP remaining is relatively constant. However, upon the addition of either the support alone (TiO$_2$) or commercial AuNP@TiO$_2$, CHP is rapidly consumed.

HPLC analysis of the reaction mixture when TiO$_2$ alone was used illustrates phenol as the main decomposition product, obtained via an ionic pathway, not a free-radical pathway.[27] The formation of phenol from CHP is largely dependent on the acidity of the TiO$_2$. Solomon and Murray[28] have shown that hydrated clays (<6% water content) effectively catalyze the formation of phenol from CHP. When the water content is
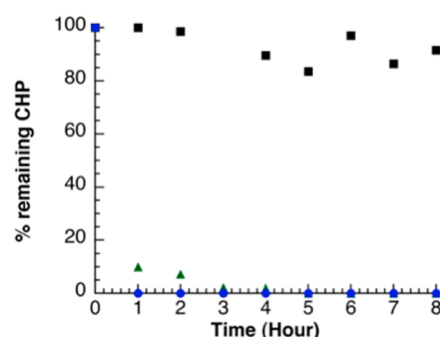

Figure 4. Decomposition of cumene hydroperoxide using no catalyst (■), TiO$_2$ only (▲), and commercial AuNP@TiO$_2$ (●) at 80 °C.

above this value, no CHP decomposition is observed. Similar experiments were conducted using TiO$_2$. In one case, the support was calcined at 400 °C for 72 h and in another was used as received. The dried TiO$_2$ sample rapidly decomposed CHP into phenol at 80 °C within 2−3 h, whereas the hydrated support remained inert toward CHP degradation (Figure S10, Supporting Information). The formation of phenol would account for the considerable CHP degradation observed in Figure 3 without detectable amounts of the expected cumyl alcohol free-radical product.

Using AuNP@HT as a Catalyst. As shown above, the radical nature of cumene hydroperoxidation ultimately requires that the hydroperoxide must be stable in the presence of the support. Of the other numerous solids tested for inertness toward CHP degradation (e.g., Al$_2$O$_3$, ZnO, clays), hydrotalcite (HT; magnesium aluminum anionic clay) was found to meet this criterion and has been shown to be inert toward radical processes.[5]

As shown in Figure 5, though cumyl alcohol is still the major product for the cumene peroxidation reaction using AuNP@
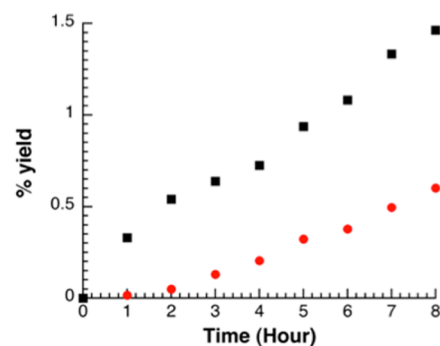

Figure 5. Percent yield of cumyl alcohol (■) and CHP (●) for AuNP@HT catalyzed cumene hydroperoxidation at 80 °C.

HT, a considerable amount of cumene hydroperoxide can be observed after 8 h of reaction. Control experiments run in the presence of HT only did not show any significant product formation (Figure S10).

The ability of HT and AuNP@HT to degrade cumene hydroperoxide was also assessed (Figure 6). Primarily, in the absence of catalyst or in the presence of HT only, CHP exhibited exceptional stability. However, when AuNP@HT was used as a catalyst, CHP degraded into cumyl alcohol, reaching a plateau after ~2 h. This plateau is likely due to the fact that the cumene hydroperoxide reagent contains about 20% cumene, which allows for a steady-state to be established between CHP
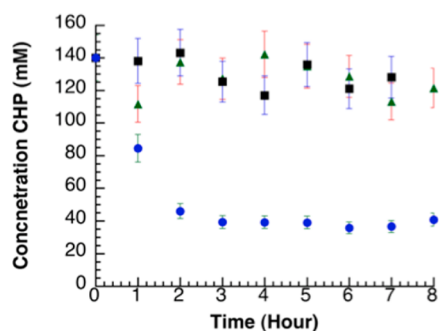
Figure 6. Decomposition of cumene hydroperoxide into cumyl alcohol using no catalyst (■), HT (▲), and AuNP@HT (●) at 80 °C.

degradation and CHP formation from cumene and atmospheric oxygen in the reaction mixture. When this reaction was carried out under inert atmosphere (N_2; Figure S11, Supporting Information), complete degradation of the CHP was observed, as the pathway for O_2-facilitated cumene hydroperoxidation was removed. The plateau observed in Figure 6 for AuNP@HT decomposition of CHP could also be partially explained by catalyst fatigue or change in the electronic properties of catalyst. A change in the properties of the catalyst may also be evidenced by the presence of a small induction time observed prior to CHP formation.

The formation and degradation of CHP using commercial AuNP@TiO$_2$ (Figures 3 and 4) and AuNP@HT (Figures 5 and 6) as catalysts illustrate that AuNP@TiO$_2$ are more active toward CHP decomposition, whereas AuNP@HT promotes the formation of CHP, the desired precursor of the aforementioned Hock rearrangement. As a nominal 1% Au loading is used for both catalysts, Au concentration must not play a large role in the observed differences in activity between AuNP@TiO$_2$ and AuNP@HT. The varying results are likely related to the difference in the size of the supported nanoparticles, where smaller particles (and, thus, more surface area) result in more efficient reaction[29] (AuNP@TiO$_2$ = 2.3 nm; AuNP@HT = 5.8 nm), as well as the effect of the support itself.[30]

Using AgNP@HT as a Catalyst. As HT is relatively inert toward CHP degradation, silver nanoparticles supported on HT (AgNP@HT) were also examined as potential catalysts for cumene peroxidation, as shown in Figure 7, for direct comparison with Au. A considerable increase in the yield of CHP with respect to cumyl alcohol can be observed in the presence of AgNP@HT, as compared with the results obtained using commercial AuNP@TiO$_2$ and HT (Figures 3 and 5,
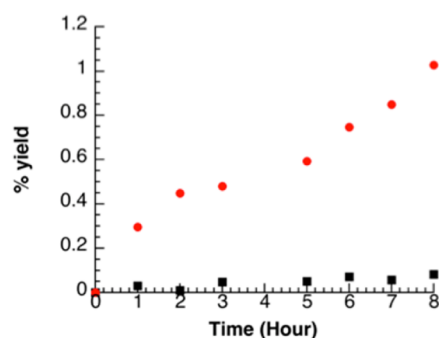

Figure 7. Percent yield of cumyl alcohol (■) and CHP (●) for AgNP@HT catalyzed cumene hydroperoxidation at 80 °C.

respectively). The amount of cumyl alcohol obtained when using AgNP@HT is minimal (0.08%) compared to 1.0% for CHP. Moreover, these results suggest very good selectivity toward CHP formation when AgNP@HT are employed as heterogeneous catalysts. The amount of cumyl alcohol obtained in the case of AgNP@HT is minimal, and the selectivity toward cumene hydroperoxide is 92% (after 8 h of reaction).

Figure 8 illustrates the ability of AgNP@HT to degrade cumene hydroperoxide and shows minimal cumene hydro-
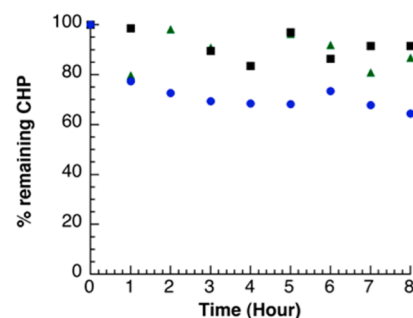

Figure 8. Decomposition of cumene hydroperoxide into cumyl alcohol using no catalyst (■), HT (▲), and AgNP@HT (●) at 80 °C.

peroxide degradation (loss of approximately 25% over 8 h) to cumyl alcohol as compared to AuNP@HT, confirming that CHP is the major product formed when supported AgNPs are used as the peroxidation catalyst.

In an attempt to increase the overall yield of cumene hydroperoxide formation, the reaction medium was saturated with oxygen (5 mL/min flow). Figure 9 shows that the overall
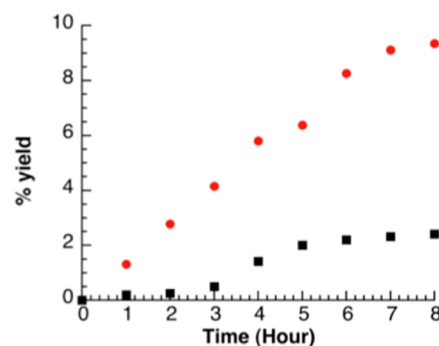

Figure 9. Percent yield of cumyl alcohol (■) and CHP (●) for AgNP@HT catalyzed cumene peroxidation at 80 °C under oxygen saturated conditions.

yield of CHP formed after 8 h of reaction was 9.4% under O_2, as compared to 1.0% under atmospheric conditions. Furthermore, the percent yield of cumyl alcohol was also found to increase from 0.08% to 2.4% in the presence of oxygen.

Table 1 summarizes the percent yields of cumyl alcohol and CHP obtained under the different reaction conditions discussed herein, as well as toward CHP formation when using supported Au and AgNP as catalysts. Importantly, in the absence of any catalytic material, no significant conversion of cumene to CHP was observed. The reaction was also carried out over a period of 24 h, yielding 18.4% CHP and 4.8% cumyl alcohol for a combined conversion of ~25%. This value is within the range of yields commonly obtained in industry.[31]

Table 1. Product Distribution and Selectivity of Au and AgNP Catalyzed Cumene Peroxidation after 8 h of Reaction at 80°C

catalyst	% yield cumyl alcohol	% yield CHP	selectivity CHP (%)
AuNP@HT[a]	0.9	0.3	25%
AgNP@HT[a]	0.1	1.0	92%
No catalyst[a]	0.0	0.03	100%
HT[a]	0.0	0.01	100%
AgNP@HT[b]	2.4	9.4	80%
No catalyst[b]	0	0.1	100%
HT[b]	0.2	1.8	80%

[a]Atmospheric conditions. [b]Oxygen saturated conditions.

Recyclability Study. The recyclability of AuNP@HT and AgNP@HT under atmospheric and oxygen saturated conditions is presented in Figure 10. After AuNP@HT is recycled
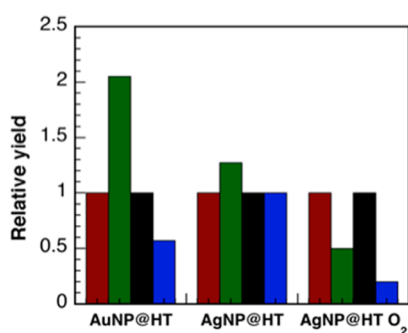
Figure 10. Recyclability experiments after one reuse of AuNP@HT and AgNP@HT (under atmospheric and oxygen saturated conditions): CHP first cycle (red), CHP second cycle (green), cumyl alcohol first cycle (black), and cumyl alcohol second cycle (blue).

once, a twofold increase in the amount of CHP and a corresponding decrease in the yield of cumyl alcohol was observed. The observed decrease in the obtained yields of cumyl alcohol can be attributed to catalyst fatigue with regard to the efficiency of the material to degrade CHP and can be used to justify the plateau of CHP decomposition observed in Figure 6. When using AgNP@HT as a catalyst under atmospheric conditions, similar yields of CHP and cumyl alcohol are obtained after one reuse, illustrating reasonable stability of the nanocomposite. However, recycling experiments using AgNP@HT under oxygen-saturated conditions illustrate deactivation of the catalyst with respect to both CHP and cumyl alcohol formation. This observation occurs in conjunction with a considerable change in the visual color of the catalyst from yellow to blue/black. Characterization of the catalyst by TEM analysis shows reduced pore stability of the HT support under these conditions (Figure S12, Supporting Information). Notably, TEM images depict the disappearance of the two-dimensional, layered structure of the HT. XPS analysis of the supported AgNP (Figure S13, Supporting Information) also illustrates some oxidation of the nanoparticles under these reaction conditions.

Oxygen Uptake Experiments. The oxygen uptake apparatus was used to evaluate the mechanism of AuNP-mediated cumene peroxidation. This methodology has been widely utilized and is well described in the literature.[32] Oxygen uptake kinetics for the free-radical cumene autoxidation is well studied with known rate constants for each elementary step.[33]

The purpose of these experiments is to compare cumene peroxidation using supported AuNP with the previously published results for the standard free-radical autoxidation of cumene.

The basic oxygen uptake experiment is described as follows: The oxygen uptake apparatus can be used to determine the rate at which oxygen is consumed by a reaction, effectively probing the propagation step. Figure 11 shows representative data
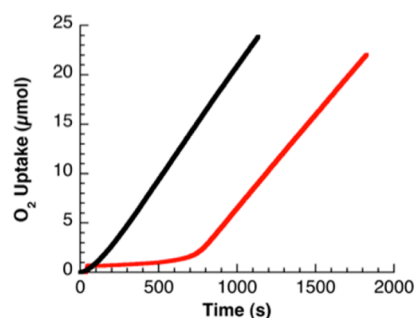
Figure 11. Typical oxygen uptake traces obtained for commercial AuNP@TiO$_2$-catalyzed cumene peroxidation using *tert*-butyl hydroperoxide as an initiator. The black line represents actual experimental data obtained and was used to calculate the amount of O$_2$ consumed as a function of time, and the red line represents actual experimental data using an antioxidant to calculate the rate of initiation.

obtained from the oxygen uptake apparatus when monitoring cumene peroxidation, where the slope of the black trace can be used to calculate the rate of propagation, R_p, equivalent to the rate at which oxygen is consumed (see Supporting Information for more details). The red trace represents an experiment where an antioxidant is added to the reaction mixture resulting in an induction period that can be used to determine the rate of initiation (R_i). The antioxidant prevents the propagation by trapping the radical species that are formed in the initiation step.

Our oxygen uptake apparatus cannot be used at elevated temperatures (maximum 30 °C). Under these experimental conditions, AuNP and AgNP@HT showed limited catalytic activity toward the peroxidation process; therefore studies were concentrated on the use of commercial AuNP@TiO$_2$. Control experiments carried out in the absence of *tert*-butyl hydroperoxide initiator and in the presence of TiO$_2$ revealed no evidence of oxygen uptake. The rate of oxygen consumption (R_p) catalyzed in the commercial AuNP@TiO$_2$ experiment was calculated to be ~1.0 × 10^{-5} M/s and decreased as the reaction progressed. The amount of oxygen consumed by the peroxidation reaction was, as expected, equivalent to the sum of cumyl alcohol and cumene hydroperoxide produced (Figure 12).

The R_i for cumene peroxidation in the presence of supported AuNP and an antioxidant was also calculated and found to be ~1.7 × 10^{-7} M/s. The equations used for the calculation of R_p and R_i can be found in the Supporting Information. From these values, the average length of the free-radical chain reaction, R_p/R_i, can also be predicted and was determined to be ~58. In principle, this number reflects the ratio between the amount of CHP and cumyl alcohol formed, as CHP is formed in the propagation step and cumyl alcohol is in the initiation step. Thus, R_p/R_i should be proportional to [CHP]/[cumyl alcohol].

Aliquots taken from the reaction cells were analyzed *via* HPLC to determine the product distribution ratio obtained
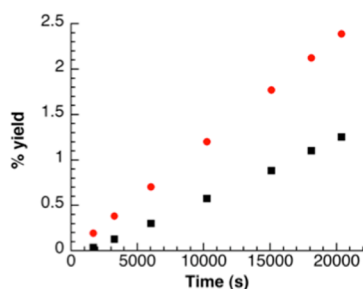
Figure 12. Percent yield of cumyl alcohol (■) and CHP (●) for cumene peroxidation using AuNP@TiO$_2$ at 30 °C using the oxygen uptake technique.

from the oxygen uptake experiments (Figure 12). The differences in percent yield values shown in this graph as compared to Figure 3 can be attributed to inherent reaction conditions of the oxygen uptake apparatus as compared to those carried out on the bench. These data indicate that the experimental value of [CHP]/[cumyl alcohol] is slightly less than 2, clearly lower than the determined free-radical chain length of 58. This discrepancy will be used to further discuss the potential mechanism for AuNP-mediated cumene peroxidation (*vide infra*).

■ DISCUSSION

Free-radical cumene peroxidation can be described as a typical chain reaction, including initiation, propagation, and termination steps. From the results obtained in this work, especially the decomposition of cumene hydroperoxide into cumyl alcohol, it is evident that both AuNP and AgNP have a significant influence on the initiation step. This decomposition can be attributed to a Fenton-like reaction in the presence of metal nanoparticles, as has been previously reported for H$_2$O$_2$ decomposition by AgNP[34] and also by AuNP supported on nanodiamond.[35]

As this work was carried out using heterogeneous catalysts, the role of the support must be considered. Previous results obtained for the peroxidation of cyclohexane using various supported AuNP, notably AuNP@TiO$_2$, attributed the majority of cyclohexane hydroperoxide decomposition to the presence of the nanoparticles.[8] However, further studies suggested that the support itself could also be responsible for some hydroperoxide decomposition when using Au@nano-CeO$_2$.[16] In the case of the work discussed herein, the results obtained when using AuNP and AgNP@HT show that the nanoparticles are mainly responsible for the decomposition of CHP into cumyl alcohol. This is evident when HT alone is used as the catalyst and minimal CHP decomposition was observed. However, in experiments where commercial AuNP@TiO$_2$ was used as a catalyst, the nature (i.e., hydration) of the support played a more important role on CHP stability. Furthermore, the major product obtained (phenol) for CHP decomposition when using TiO$_2$ alone supports an acid-catalyzed mechanism, rather than a free-radical pathway.[36]

When considering the pathways responsible for supported nanoparticle-catalyzed cumene peroxidation, it is important to consider past literature precedents.[34,35,37] Both Au and Ag nanoparticles actively decompose hydroperoxides *via* a Fenton-like reaction. As such, the initial step in our schematic representation, presented in Figure 13, involves the adsorption of hydroperoxide (either the *tert*-butyl hydroperoxide initiator or cumene hydroperoxide formed throughout the reaction) onto the NP surface and a subsequent Fenton cleavage to result in RO• and HO⁻. The possibility of a homogeneous catalysis caused by catalytic leaching of supported AuNP into the reaction mixture was also considered, as such a pathway would lead to Fenton chemistry happening in solution. However, no Au could be detected following ICP analysis of the catalytic reaction mixture after the removal of the catalyst by centrifugation, ruling out such a possibility. Following the initial Fenton cleavage of the hydroperoxide via the adsorption of ROOH onto the nanoparticle surface, the nanoparticle-
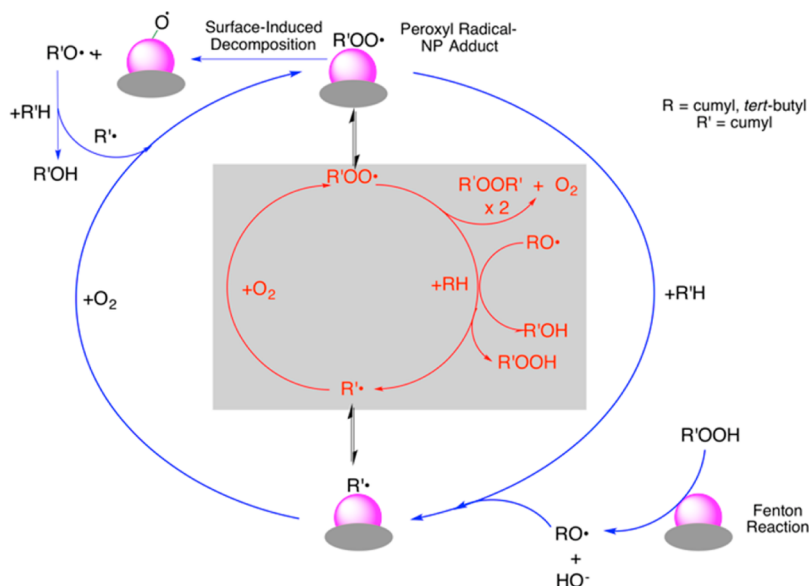

Figure 13. Schematic representation of cumene peroxidation in the presence of metallic nanoparticles. Blue arrows are representative of reactions occurring on the nanoparticle surface, while red arrows indicate pathways within the bulk solution. The red pathway enclosed in a gray box is well established in solution; such homogeneous autoxidation is a slow process at the temperatures used in this work, but this may be largely due to inefficient homogeneous initiation.

catalyzed peroxidation of cumene can be thought of as involving a combination of radical reactions occurring in solution and on the nanoparticle surface. The reactions occurring on the nanoparticle surface could influence any of the steps of the free-radical mechanism shown in eqs 1−4, either while on the surface or through exchange between the surface and the solution. Only the initiation (reaction 1) is likely unimportant in the solution phase at 80 °C, while other steps may be viable in either phase. For example, considering that the reaction rate constant between carbon-centered radicals and oxygen is close to diffusion-controlled (10^9 M^{-1} s^{-1}),[38] it would be unlikely for the step involving reaction between the cumyl radical and oxygen to be more efficient on the nanoparticle surface, as it is already the dominant pathway for cumyl radicals.

In this work and under the presence of oxygen, the radical that interacts with the gold surface is likely an oxygen-centered radical, either alkoxyl or peroxyl in nature, derived from the cumyl radical. Thus, following the formation of RO$^\bullet$ via Fenton chemistry, H-abstraction from a molecule of cumene results in the formation of a cumyl radical and cumyl alcohol. Subsequent reaction between the cumyl radical and O_2 gives rise to cumyl peroxyl radicals as the main intermediates. It is important to note that adsorption of oxygen-centered radicals onto the nanoparticle surface is considered a rapid process,[39] though competition with the H-abstraction pathway in solution cannot be dismissed. Aprile et al. also have suggested the formation of a similar type of peroxyl radical-AuNP adduct.[40]

Once formed, the possible fate of the cumyl peroxyl radical-nanoparticle adduct is twofold. First, the binding between the nanoparticle surface and the peroxyl radical may be reversible and simply go back into solution. This intermediate could then undergo either (1) H-abstraction from an additional molecule of cumene, forming cumene hydroperoxide and cumyl alcohol, or (2) a termination step to form dicumyl peroxide (DCP). This is supported by the small amounts of DCP illustrated in Figure 3, when commercial AuNP@TiO$_2$ are employed as the reaction catalyst, and corroborates the presence of a solution-based pathway.

The second possibility involves surface-induced decomposition of the cumyl peroxyl radical-nanoparticle adduct (see top-left in Figure 13); this pathway ultimately generates a molecule of cumyl alcohol and a radical R$^\bullet$ that re-enters the autoxidation reaction. Though H-abstraction can still possibly yield CHP, evidence for surface decomposition of peroxyl radical-nanoparticle adducts has been previously observed.[41] From the aforementioned findings, O−O bond cleavage is favored over Au−O dissociation for methyl peroxyl radical adducts.[41] In the context of Figure 13, this would result in the formation of Au−O$^\bullet$ and RO$^\bullet$, yielding cumyl alcohol as the final product. Similar Au−O species have been recently predicted as active participants in the interaction of AuNP with oxygen and hydrocarbons.[42]

The oxygen uptake experiments can be used to support the formation of cumyl alcohol by a pathway other than the initial hydroperoxide decomposition, as shown to the right of Figure 12. The free-radical chain length was predicted to be ∼58. Recalling that this value (R_p/R_i) is proportional to [CHP]/[cumyl alcohol], if the only mechanism for the formation of cumyl alcohol was nanoparticle-catalyzed CHP decomposition, the calculated [CHP]/[cumyl alcohol] should be similar to the predicted value. However, the calculated chain length from analysis of HPLC product distribution was ∼2. This suggests

that the concentration of cumyl alcohol is considerably larger than originally predicted and indicates that an additional nanoparticle-induced pathway may be responsible for alcohol formation. One such possibility entails the surface induced decomposition of cumyl peroxyl radicals. Unfortunately, oxygen uptake reactions are limited to 30 °C; therefore further experiments were carried out to support the suggested participation of free radicals in solution, as well as nanoparticle surface chemistry in the mechanism presented in Figure 13. 2,6-Di-tert-butyl-4-methoxyphenol (DBHA) was added 1 h after the reaction to trap any free-radical species in solution. For AuNP@HT (Figure S18) and AuNP@TiO$_2$ (Figure S19), the addition of DBHA resulted in the inhibition of the product formation over the remaining course of the experiment. These results demonstrate that, at 80 °C, supported AuNP catalyzed cumene peroxidation does involve the participation of solution free-radical species. Lipoic acid was also added as a probe in order to get a better understanding of the involvement of the nanoparticle surface, due to the inherently strong interactions between the AuNP and sulfur.[43] Ideally, lipoic acid will interact and cap the AuNP surface preventing the surface decomposition of peroxyl radical into the corresponding alkoxyl radical and decreasing the yield of cumyl alcohol observed. Figures S21 and S22 show the effects of lipoic acid addition to reactions using AuNP@HT and AuNP@TiO$_2$ as catalysts, respectively. In both cases, lipoic acid appears to halt and plateau the formation of CHP and cumyl alcohol, thus supporting the role of the gold nanoparticle surface in the formation of cumyl alcohol via peroxyl radical surface decomposition. It is important to note that given the known contribution of solution free-radical chemistry within the proposed peroxidation mechanism, a complete prevention of CHP and cumyl alcohol formation is not expected but more so a plateau of the product yields, as is observed.

AgNP@HT can be suggested to be a superior catalyst, as the largest yields of the desired CHP product are obtained when this material is used in the reaction. However, even though both AgNP@HT and AuNP@HT exhibit cumene peroxidation ability, a generalized comparison between the two should not be made due to the differences in both size and nature of the metal nanoparticles. Unfortunately, oxygen uptake experiments could not be carried out using the AgNP@HT catalyst due to a lack of activity under the operating conditions of the instrument (i.e., 30 °C). Therefore experiments with DBHA (Figure S20) and lipoic acid (Figure S23) at 80 °C, similar to those undertaken for the supported AuNPs, were performed. The addition of DBHA showed a decrease in the yields of both CHP and cumyl alcohol indicating an inhibition of free radical chemistry in solution. Lipoic acid has also demonstrated the ability to protect and cap the AgNP surface.[44] The addition of lipoic acid to the peroxidation reaction using AgNP@HT as a catalyst resulted in a reduction in CHP and cumyl alcohol formation demonstrating involvement of the AgNP surface in the peroxidation mechanism. Given these results, the formation of a peroxyl radical-nanoparticle adduct cannot be dismissed. In principle, the surface decomposition of a peroxyl radical-AgNP adduct must be a less favored pathway or, at least, more reversible when AgNP@HT are used, as CHP is the product.

Reflecting on the two questions posed within the Introduction, the following statements can be made from the present study. First, when considering the ability of Au and AgNP to decompose hydroperoxides, the HPLC product distribution data clearly show this is the case, where AuNP

initiates CHP degradation more rapidly than the corresponding Ag composites. Specifically, cumyl alcohol was determined to be the major product when supported AuNP's were used, while CHP was the major product for the supported AgNP-catalyzed cumene peroxidation reaction.

In regard to the second question posted, both supported Au and AgNP were found to influence the kinetics of the peroxidation reaction. In the absence of supported nano-particles at 80 °C, minimal peroxidation products were observed after 8 h, but addition of the heterogeneous nanoparticle catalyst increased the yields of both CHP and cumyl alcohol formed with the reaction mixture. The formation of the proposed peroxyl radical-nanoparticle adduct would be expected to play an important role in the kinetics of this reaction.

CONCLUSION

Peroxidation of cumene was studied at low conversions due to the interest in understanding the oxidation reaction using supported metal nanoparticles, as this reaction is considerably important from an industrial point of view. Both the role of the support and that of the nanoparticle were investigated, where the influence of the supported nanoparticles was considerably more important with respect to CHP degradation and cumene peroxidation than support participation in the reaction. The nature of the supported nanoparticle has a major influence on the overall product distribution, with supported AuNP yielding cumyl alcohol as the major product, and CHP when supported AgNP were used. When using supported AuNP, the cumyl alcohol product may have two origins, one through Fenton-induced decomposition of hydroperoxides and a second through surface-induced decomposition of a proposed peroxyl radical-nanoparticle adduct.

ASSOCIATED CONTENT

Ⓢ Supporting Information

TEM data for AuNP and AgNP@HT, representative HPLC data, kinetics for cumene peroxidation control experiments, kinetics for CHP decomposition data using hydrated and dried TiO_2 P25, kinetics for CHP decomposition under N_2 using AuNP@HT, description of oxygen uptake apparatus, and methodology used for data interpretation. This material is available free of charge via the Internet at http://pubs.acs.org.

AUTHOR INFORMATION

Corresponding Author
*E-mail: scaiano@photo.chem.uottawa.ca (J.C.S.), josecarlos@photo.chem.uottawa.ca (J.C.N.-F.).

Notes
The authors declare no competing financial interest.

ACKNOWLEDGMENTS

REFERENCES

(1) Weissermel, K.; Arpe, K. J. *Industrial Organic Chemistry*, 4th ed.; Wiley-VCH: Darmstadt, Germany, 2003.
(2) Kamir, Y.; Beaton, S.; Lafortune, A.; Ingold, K. U. *Can. J. Chem.* **1963**, *41*, 2020−2033.
(3) Woodward, A.; Mesrobian, R. B. *J. Am. Chem. Soc.* **1953**, *75*, 6189−6195.
(4) Varma, G. R.; Graydon, W. F. *J. Catal.* **1973**, *28*, 236−244.
(5) Jana, S. K.; Wub, P.; Tatsumi, T. *J. Catal.* **2006**, *240*, 268−274.
(6) Casemier, J. H. R.; Nieuwenhuys, B. E.; Sachlter, W. M. H. *J. Catal.* **1973**, *29*, 367−373.
(7) Richardson, W. H. *J. Am. Chem. Soc.* **1965**, *87*, 1096−1102.
(8) Hereijgers, B. P. C.; Weckhuysen, P. M. *J. Catal.* **2010**, *210*, 16−25.
(9) Xu, Y. J.; Landon, P.; Enache, D.; Carley, A. F.; Roberts, M. W.; Hutchings, G. J. *Cat. Lett.* **2005**, *101*, 175−179.
(10) Liu, Y.; Tsunoyama, H.; Akita, T.; Xie, S.; Tsukuda, T. *ACS Catal.* **2011**, *1*, 2−6.
(11) Zhoua, H. J.; Luoa, H.; Zenga, C.; Lia, D.; Liu, Y. *Cat. Lett.* **2006**, *108*, 49−55.
(12) Centi, G.; Perathoner, S.; Trifiro, F. *Sustainable Industrial Chemistry*; Wiley-VCH: Weinheim, Germany, 2009.
(13) Van Ham, N. H. A.; Nieuwenhuys, B. E.; Sachtler, W. M. H. *J. Catal.* **1971**, *20*, 408−423.
(14) Panayotava, E. N.; Dimitrov, D. I.; Petkov, A. A. *J. Catal.* **1976**, *41*, 329−332.
(15) Zu, S.; Hang, C.; Zhang, J.; Chen, B. *Korean J. Chem. Eng.* **2009**, *26*, 1568−1573.
(16) Lloyd, R.; Jenkins, R. L.; Piccinini, M.; He, Q.; Kiely, C. J.; Golunski, S. E.; Bethell, D.; Bartley, J. K.; Hutchings, G. J. *J. Catal.* **2011**, *283*, 161−167.
(17) Goszner, K.; Bischof, N. *J. Catal.* **1974**, *32*, 175−182.
(18) Navalon, S.; de Miguel, M.; Martin, R.; Alvaro, M.; Garcia, H. *J. Am. Chem. Soc.* **2011**, *133*, 2218−2226.
(19) Schmidt, R. J. *Appl. Catal., A* **2005**, *280*, 89−103.
(20) Mitsudome, T.; Noujima, A.; Mizugaki, T.; Jitsukawa, K.; Kaneda, K. *Adv. Synth. Catal.* **2009**, *351*, 1890−1896.
(21) Mitsudome, T.; Mikami, Y.; Funai, H.; Mizugaki, T.; Jitsukawa, K.; Kaneda, K. *Angew. Chem., Int. Ed.* **2008**, *47*, 138−141.
(22) Howard, J. A. *Advances in Free Radical Chemistry*; Logos Press: London, England, 1972; Vol. 4.
(23) Fillippenko, V. *Oxygen Uptake Studies of Organic and Inorganics Oxidations*; MSc Thesis, University of Ottawa, Ottawa, Ontario, Canada, 2010.
(24) Barclay, L. R. C.; Vinqvist, M. R. *Free Radic. Biol. Med.* **1994**, *16*, 779−788.
(25) Kharasch, M. S.; Fono, A.; Nudernberg, W. *J. Org. Chem.* **1949**, *14*, 763−774.
(26) Barrett, K. E.; Thomas, H. R. *J. Polym. Sci., Polym. Chem.* **1969**, *7*, 2621−2650.
(27) Kharasch, M. S.; Fono, A.; Nuderberg, W. *J. Org. Chem.* **1949**, *14*, 748−752.
(28) Solomon, D. H.; Murray, H. M. *Clays Clay Miner.* **1972**, *20*, 135−141.
(29) Corma, A.; Garcia, H. *Chem. Soc. Rev.* **2008**, *37*, 2096−2126.
(30) Naya, S.-i.; Teranishi, M.; Kimurab, K.; Tada, H. *Chem. Commun.* **2011**, *47*, 3230−3232.
(31) Chauvel, A.; Lefebre, G. G. *Petrochemical Processes: Technical and Economic Characteristic*; Ophrys: Paris, 1989; Vol. 2.
(32) Barclay, L. R. C.; Ingold, K. U. *J. Am. Chem. Soc.* **1981**, *103*, 6478−6485.
(33) Howard, J. A.; Ingold, K. U. *Can. J. Chem.* **1968**, *46*, 2555−2660.
(34) Jones, A. M.; Garg, S.; He, D.; Pham, A. N.; Waite, T. D. *Environ. Sci. Technol.* **2011**, *45*, 1428−1434.
(35) Navalon, S.; Martin, R.; Alvaro, M.; Garcia, H. *Angew. Chem., Int. Ed.* **2010**, *49*, 8403−8407.
(36) Salukvadze, L. V.; Norikov, Y. D.; Valendo, A. Y.; Blyumberg, E. A. *Russ. Chem. Bull.* **1972**, *7*, 1478−1482.

(37) Della Pina, C.; Falletta, E.; Prati, L.; Rossi, M. *Chem. Soc. Rev.* **2008**, *37*, 2077−2095.

(38) Maillard, B.; Ingold, K. U.; Scaiano, J. C. *J. Am. Chem. Soc.* **1983**, *105*, 5095−5099.

(39) Menchon, C.; Martin, R.; Apostolova, N.; Victor, V. M.; Alvaro, M.; Herance, J. R.; Garcia, H. *Small* **2012**, *8*, 1895−1903.

(40) Aprile, C.; Corma, A.; Domine, M. E.; Garcia, H.; Mitchell, C. *J. Catal.* **2009**, *264*, 44−53.

(41) Bar-Ziv, R.; Zilbermann, I.; Zidki, T.; Cohen, H.; Meyerstein, D. *J. Phys. Chem. C.* **2009**, *113*, 3281−3286.

(42) Boronat, M.; Corma, A. *J. Catal.* **2011**, *284*, 138−147.

(43) Brust, M.; Walker, M.; Bethell, D.; Schiffrin, D. J.; Whyman, R. *J. Chem. Soc., Chem. Commun.* **1994**, 801−802.

(44) Gan, W.; Xu, B.; Dai, H. L. *Angew. Chem., Int. Ed.* **2011**, *50*, 6622−6625.